Analytical Analysis of the Accuracy of HYPR LR in CE MRA

H. Wu[1], A. A. Samsonov[2], J. Velikina[2], and W. F. Block[3]

[1]Medical Physics, University of Wisconsin-Madison, Madison, Wisconsin, United States, [2]Radiology, University of Wisconsin-Madison, United States, [3]Biomedical Engineering, University of Wisconsin-Madison, United States

Introduction: Image acceleration methods, such as Highly constrained Back Projection (HYPR) [1], have recently been of significant interest due to their capabilities for capturing dynamic events with MRI. However, the non-linear nature of these methods has made characterizing their accuracy difficult with analytical methods and thus simulations have been primarily utilized [2]. The formulation of the newer method known as HYPR Local Reconstruction (HYPR LR) [3], which focuses on local objects, allows an analytical approach which can predict reconstruction accuracy for commonplace objects often found in contrast-enhanced MR angiography (CE-MRA). In this work, we derive expressions predicting the accuracy of HYPR LR for spatially adjacent objects in the presence of changing background tissue and verify the behavior in digital and in vivo experiments.

Theory: The HYPR-LR algorithm is described by the following formula:

$$I_{LR}(\bar{r},t) = I_C(\bar{r}) \cdot \frac{I_t(\bar{r},t) \otimes k(\bar{r})}{I_C(\bar{r}) \otimes k(\bar{r})} \qquad (Eq.1)$$

, where I_C is the time-averaged image, $k(\bar{r})$ is a convolution kernel, and I_t is an estimated image of a shorter, individual time frame. For illustrative purposes, we derive the HYPR LR output for a 1D function modeling common CE-MRA objects, though extending the derivation to 2D or 3D objects is straight forward. The object consists of a time-varying artery, $a(r,t)$, a vein $v(r,t)$ and background $b(r,t)$, shown in Fig. 1a. Though not necessary for the derivation but in order to simplify the output expression, we assume that temporal and spatial behavior for each object are separable (e.g. $a(r,t) = a(r)\ a(t)$), the amplitude does not vary across the objects, and the DC gain of $k(r)$ is 1 and thus the area under the curve $k(r)$ =1. We denote the mean temporal signal of the artery, vein, and background by A,V, B, respectively.

Under such assumptions, the contents of the numerator and denominator in equation 1 can be viewed as the superposition of three individual convolution operations between the kernel and the artery, vein, and background. The output of each convolution at the location r is the product of the amplitude of the object and the area it subtends under a shifted k(r), as shown in Fig. 1b, where the shift depends on the desired output location r. We denote the area subtended by artery by w_a ,

$$I_{LR}(r,t) = I_c(r) \cdot \frac{I(r,t) \otimes k(r)}{I_c(r) \otimes k(r)} = [Aa(r) + Vv(r) + Bb(r)] \cdot \frac{w_a a(t) + w_v v(t) + (1 - w_a - w_v) b(t)}{w_a A + w_v V + (1 - w_a - w_v) B} \qquad (Eq.2) \qquad where\ w_a = \int_{-r}^{r_1 - r} k(r)dr,\ w_v = \int_{r_2 - r}^{r} k(r)dr$$

shown in red in Fig. 1b, and the area subtended by the vein by w_v, shown in blue in Fig. 1b. The HYPR LR output can then be written as:

$$a(r,t) = \frac{w_a a(t) + w_v v(t) + (1 - w_a - w_v) b(t)}{w_a + w_v \frac{V}{A} + (1 - w_a - w_v) \frac{B}{A}} = \frac{w_a a(t) + w_v v(t) + (1 - w_a - w_v) b(t)}{g(r)} \qquad (Eq.3)$$

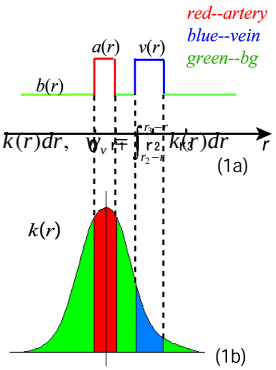

Figure 1. 1D object model and convolution kernel with w_a shown as red area, w_v as blue area

To further simplify the output, we consider the output only over the region of the artery and scale the output by the mean arterial signal A.

The expression in Eq. 3 predicts that the actual arterial waveform will be dampened, as well as offset by the venous and background signal. The dampening coefficient, $w_a/g(r)$, depends on the ratio of the subtended area in w_a and the denominator $g(r)$ in Eq. 3. The function w_a has a maximum at the center of the vessel and a minimum at its edge. w_a also grows as the ratio of the width of the artery to the width of the kernel. The denominator of the ratio, $g(r)$, depends only on the mean signal statistics and varies throughout the image depending on the local venous and background structures. The venous contamination for an arterial voxel, described by w_v, increases as the distance between the arterial and venous objects decreases. The background contamination grows as the width of the artery decreases or as one moves to the edge of the artery, since w_a decreases in these situations. Contamination from the background and venous structures depends primarily on the current time frame, as shown in the numerator of Eq. 3.

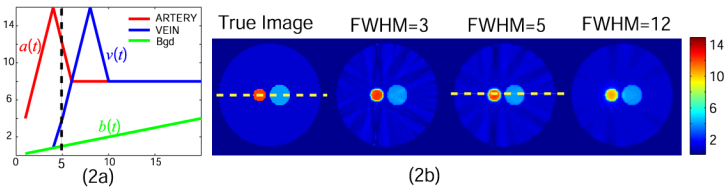

Figure 2. True waveforms of 3 objects (left) and HYPR LR images (right) reconstructed with kernels of widths: 3, 5, 12 at time point 5 (indicated by a black dashed line on the left.

Methods: We built a digital phantom consisting of a small arterial vessel (red in Fig. 2), an adjacent vein shown (blue), and enhancing background tissue (green). We assigned different temporal waveforms to the three areas (Fig. 2). A simulated acquisition consisted of 20 projections per time frame, 256 points/projection. HYPR LR reconstructions were done with a circularly symmetric kernel with FWHM of 3, 6, 12.

Results: For very small kernel sizes, contamination of vessel signal from the nearby object and background is insignificant, but streak artifacts substantially degrade image quality (Fig 2b). As the kernel widens, streaking artifacts are reduced with simultaneous increase of temporal error. The spatial deviation at time point 5 in the simulation is shown in Figure 3. The temporal deviation can be observed in the waveforms (Figure 4) for a pixel at the edge of artery closest to the vein (left) and in the center of the artery (right). As predicted by Eq 3, the arterial waveform in HYPR LR is dampening at the arterial edge. Background contamination grows in the later time frames as the background increases in intensity. Distortion in the center of the artery, shown on the right of Fig. 4, is insignificant, as also predicted by Equation 3. Note that Equation 3 also indicates that narrowing the kernel width has limited effect in decreasing waveform distortion at the edge of the arterial voxel.

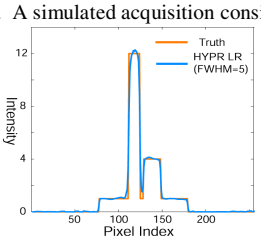

Figure 3. Comprarison of the true and HYPR LR profiles

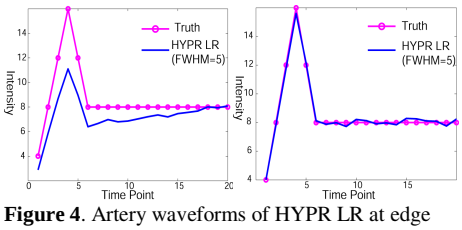

Figure 4. Artery waveforms of HYPR LR at edge pixel (left) and at center pixel (right).

Conclusion: An analytical prediction of the temporal and spatial accuracy for HYPR LR has been presented for objects common in CE-MRA. The prediction agrees with intuitive reasoning and digital simulations, and demonstrates the importance of sparsity and background suppression as acceleration factors increase. The predicted behavior also agrees generally with our clinical experience, though further work is necessary to create an experimental model to quantitatively verify the expression.

Acknowledgments: This research is supported NCI R01CA116380 and GE Healthcare.

References: [1] Mistretta et al. MRM, 55:30-40 (2006). [2] Johnson et al. MRM, 59:456-462 (2008).